Interfacial Dzyaloshinskii-Moriya Interaction, Perpendicular Magnetic Anisotropy and damping in CoFeB/oxide-based systems

I. Benguettat-El Mokhtari [1,2], Y. Roussigné[1], S. M. Chérif[1], S. Auffret[3], C. Baraduc[3], H. Béa[3] and M. Belmeguenai[1]

[1] Université Sorbonne Paris Nord, LSPM, CNRS, UPR 3407, F-93430 Villetaneuse, France
[2] LPCMME, Université Oran1, BP1524, El M'naouar 31100 Oran, Algérie
[3] Université Grenoble Alpes, CEA, CNRS, Grenoble INP, IRIG, SPINTEC, F-38000 Grenoble, France

Perpendicular magnetic anisotropy (PMA), spin pumping induced damping and interfacial Dzyaloshinskii-Moriya interaction (iDMI), which are spin-orbit coupling-related phenomena of utmost importance for applications, were experimentally investigated in as grown and 225°C annealed CoFeB/PtO$_x$, CoFeB/TaO$_x$ and Ta/CoFeB/TaOx systems by means of vibrating sample magnetometry, microstrip ferromagnetic resonance and Brillouin light scattering techniques. By varying Co$_8$Fe$_{72}$B$_{20}$ (CoFeB) thickness in the range 0.8-10 nm, the effect of Ta buffer layer on anisotropy and damping was first studied, where a large surface magnetic anisotropy (K$_s$=2.1±0.16 erg/cm^2) was measured in the unbuffered CoFeB/TaOx(0.8nm) system most likely due to their higher roughness induced by the substrate. K$_s$ degrades significantly for CoFeB film thickness below 2 nm where spontaneous perpendicular magnetization was found to be impossible without Ta buffer layer. PMA, iDMI and damping of as-deposited and 225°C annealed CoFeB(1.5 nm)/PtO$_x$ systems were measured as a function of PtO$_x$ thickness in the range 0.7-1.6 nm. Their strong dependence versus the PtO$_x$ thickness was attributed to the decrease of the magnetic dead layer as PtO$_x$ thickness increases. Linear dependence of damping versus PMA constant were obtained confirming their relation with the spin orbit coupling. Moreover, annealing increases PMA and the effective mixing conductance probably due to the enhancement of the CoFeB crystal structure and interfaces.

Index Terms— **Ferromagnetic resonance, interfacial Dzyaloshinskii-Moriya interaction, magnetic damping, magnetic anisotropy,**

I. INTRODUCTION

SINCE THE DISCOVERY of the giant magnetoresistance effect [1,2], extensive efforts have been devoted to the development of spintronics, where devices use in addition to the charge of the electron its quantum property spin, unlike conventional electronic semiconductors. Smaller, faster and efficient, these words describe the features of spintronics devices for data storage [3], including nonvolatility, high speed and low power consumption. Magnetic tunnel junction (MTJ) [4], and the skyrmions racetrack memory [5, 6], remain the most promising spintronic devices. However, it was found that realizing such high-performance spintronic devices, is quite dependent on multilayers based systems where heavy-metal (HM)/ferromagnetic (FM) interface play a crucial role. Indeed, spin-orbit coupling (SOC)-related phenomena at HM/FM interface, such as perpendicular magnetic anisotropy (PMA) [7], spin pumping [8, 9], and interfacial Dzyaloshinskii-Moriya interaction (iDMI) [10, 11], are the most interesting.

PMA materials are one of the best candidates for magnetic storage. Indeed, it enhances thermal stability and induced low driving current in Magnetic random access memory (MRAM) [12], where MTJ is the unit cell. PMA was found to exist at HM/FM [7] and also in FM/Metal Oxide (MO$_x$) interface [13, 14]. Among PMA materials, CoFeB/MgO-based structures are widely studied, due to their high tunnel magnetoresistance [15,

16] and low magnetic damping [16, 17]. However, to improve MTJ performance, thermal stability is still the major issue. Since then, plenty of endeavors have been put to find the best CoFeB-based structure showing strong PMA, by investigating various HM and MO$_x$ materials [14].

Besides PMA, "iDMI", another SOC effect is also widely investigated for the future spintronic devices to encode bits. Indeed, iDMI which is an antisymmetric exchange interaction, combined with PMA can give rise to a variety of chiral magnetic textures such as spin spirals [18, 19] and skyrmion lattices [20, 21]. A sufficiently large iDMI can also stabilize chiral domain walls [22]. Knowing that the existence of the iDMI requires the broken inversion symmetry, the large SOC at HM/FM interface also play determining role since it favors significant iDMI following the Fert-Levy model [21]. Therefore, considerable effort has been made to search for materials with large DMI or new possibilities to enhance DMI for the skyrmion/domain wall based spintronic devices. Until recently, the iDMI investigation focused on the FM/HM interface, nevertheless it can also exist at FM/Oxide interfaces attributed to the Rashba interfacial coupling [23], which was analyzed from theoretical studies [23, 24] and lately demonstrated experimentally [25, 26]. However, the understanding of the physical triggering mechanisms is still missing. Particularly, the effect of oxygen concentration and annealing combined with different metal oxides on the amplitude and sign of iDMI.

In this work, we investigated the CoFeB thickness dependence of PMA and damping in CoFeB/TaO$_x$(0.8 nm) and Ta/CoFeB/TaO$_x$(0.8 nm), where a large perpendicular surface anisotropy was found for CoFeB/TaO$_x$(0.8 nm). We also demonstrate the possibility of tuning and controlling iDMI, PMA and spin pumping induced damping in CoFeB(1.5

nm)/PtO$_x$ by varying the PtO$_x$ thickness and the oxidation level in as grown and 225°C annealed samples. This allowed understanding PtO$_x$ effect on these three effects. For this, Brillouin light scattering (BLS), ferromagnetic resonance with microstrip line (MS-FMR) coupled to vibrating sample magnetometery (VSM) were used.

II. SAMPLES AND EXPERIMENTAL TECHNIQUES

Co$_8$Fe$_{72}$B$_{20}$/MO$_x$ bilayers, where MO$_x$=PtO$_x$ or TaO$_x$, were grown at room temperature directly on thermally oxidized silicon (Si/SiO$_2$) substrates or using 3 nm thick Ta buffer layer by DC magnetron sputtering having high base vacuum level (typically in the range of several 10^{-8} mbar). TaO$_x$ and PtO$_x$ were obtained by growing the desired Ta or Pt thickness which is then oxidized in a treatment chamber. For Ta oxidation, an oxygen pressure of 150 mbar for 10 s has been used, whereas for Pt oxidation, oxygen plasma with a power of 10 W and oxygen pressure of 3×10^{-3} mbar was used for 85 s. All the samples were further capped by Al (0.5 nm) for surface protection and in order to prevent some metallic Al to remain, which could be detrimental to gate voltage application on the stack (not shown here) [27]. To investigate the FM thickness dependence of the SOC-related phenomena and for both Ta-buffered and unbuffered samples, the CoFeB thickness (t$_{CFB}$) has been varied in ranges 0.8-10 nm and 2-10 nm for Ta/CoFeB/TaO$_x$ and CoFeB/TaO$_x$, respectively. The TaO$_x$ is kept constant (0.8 nm) and samples were then annealed at 225°C, optimized to improve PMA [28], in vacuum for 30 minutes. Note that due to the weak measured iDMI in the previously investigated Ta/CoFeB/TaO$_x$, we limited our comparison between CoFeB/TaO$_x$ and Ta/CoFeB/TaO$_x$ to evidence the effect of Ta buffer layer to PMA and damping and only samples with CoFeB in the range 2-10 nm are considered CoFeB/TaO$_x$. The second category of samples considered in this study is composed of 1.5 nm thick CoFeB grown on Si/SiO$_2$ substrate without Ta (3nm) underlayer and capped by Pt layer with variable thickness (0.7 nm ≤t$_{Pt}$≤1.6 nm). Both as grown and 225°C annealed samples are considered for this category. The deposited thicknesses are determined by the opening time of the shutter that covers the target, calibrated by recording the time deposition of 30 nm thick films, measured by x-ray reflectivity.

The magnetic moment at saturation has been determined from the hysteresis curves obtained by VSM, under in-plane applied magnetic field. MS-FMR was used to determine the gyromagnetic ratio, the damping and the PMA for the thicker films. BLS has been used to investigate PMA and iDMI. For this, Stokes (S) and anti-Stokes (aS) spin wave (SW) frequencies have been measured as function of the in-plane applied magnetic field and the SW vector (k$_{SW}$). For PMA investigation, the field dependence of the mean frequency [(F$_S$+F$_{aS}$)/2], at fixed spin SW vector of 4.1 µm^{-1} (incidence angle of 10°) was used, whereas, the variation of the frequency mismatch between S and aS lines (ΔF=F$_S$-F$_{aS}$) versus k$_{SW}$ allowed to characterize iDMI strength.

III. RESULTS AND DISCUSSIONS

A. 1- Effects of CoFeB thickness and Ta buffer layer

The Magnetization at saturation (M$_s$), the magnetic dead layer thickness (t$_d$) and the gyromagnetic ratio (γ) are needed for the precise characterization of iDMI, PMA and spin pumping efficiency. M$_s$ and t$_d$ have been deduced from the CoFeB thickness dependence of the saturation magnetic moment per unit area measured by VSM, shown in figure 1 for CoFeB/TaO$_x$, Ta/CoFeB/TaO$_x$ and CoFeB/PtO$_x$. The data indicate that M$_s$ values are 1470±50 emu/cm^3, 1536±60 emu/cm^3 [29] and 1520±50 emu/cm^3 for CoFeB/TaO$_x$(0.8nm), Ta/CoFeB/TaO$_x$(0.8nm) and CoFeB/PtO$_x$(1nm), respectively. These high values of M$_s$ are most probably due the CoFeB composition which is rich in Fe known to have high values of M$_s$. The corresponding t$_d$ are 0.71±0.16 nm, 0.7±0.1 nm [29] and 1.02±0.22 nm, respectively. This magnetic dead layer is most probably attributed to intermixing of the top Ta or Pt metals and the CoFeB layer when these top metals are not completely oxidized and to the interpenetrating oxygen atoms in CoFeB during oxidation of Ta or Pt, owing to the similar magnetic dead layer thickness of the unbuffered and Ta-buffered CoFeB/TaO$_x$ samples. This is compatible with the thicker magnetic dead layer (1 nm) for CoFeB/PtO$_x$ since Pt does not generally oxidize and therefore, the oxygen penetrates more into the CoFeB films, increasing thus the thickness of the magnetic dead layer. In the following, all parameters will be discussed as a function of this effective thickness defined as t$_{eff}$=t$_{CFB}$-t$_d$, unless if explicitly mentioned.
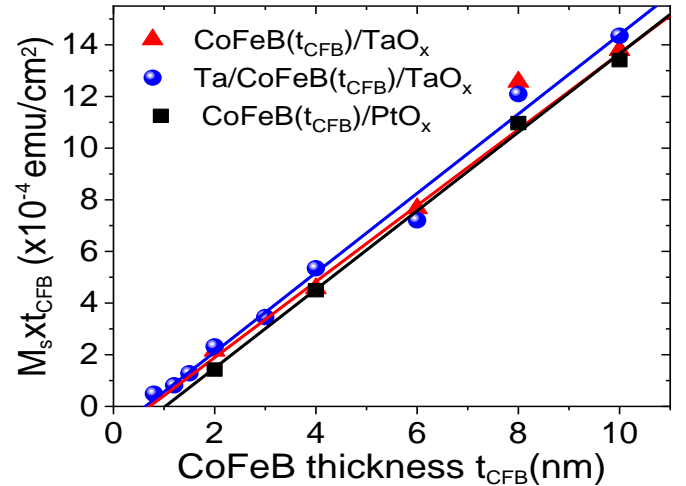

Fig. 1. Saturation magnetic moment per unit area versus thickness of the CoFeB-based systems annealed at 225° C. Symbols refer to experimental data and solid lines are linear fits.

For the gyromagnetic ratio γ and consequently the g-factor, MS-FMR under perpendicular applied magnetic field has been used to measure the applied magnetic field dependence of the uniform precession mode frequency for unbuffered and Ta-buffered CoFeB/TaO$_x$ samples [29]. The obtained values of γ/2π are 30.27±0.12 GHz/T (g=2.16±0.1) and 28.86±0.14 GHz/T (g=2.07±0.01), respectively. It is worth mentioning that the g-factor is known to be strongly influenced by surface and interface effects, as it depends on the local symmetry [30]. Therefore, it is not surprising to observe a buffer layer

dependence of g-factor.

In the next paragraph, the focus is made on the investigation of effect of Ta buffer layer on PMA by measuring the effective magnetization ($4\pi M_{eff}=4\pi M_s-2K_\perp/M_s$) for each sample of CoFeB/TaO$_x$-based systems. The perpendicular anisotropy constant ($K_\perp$) is then determined. To have $4\pi M_{eff}$, MS-FMR and BLS data, giving the in-plane applied magnetic field dependence of the uniform precession mode frequency (MS-FMR) and mean frequency (F_S+F_{aS})/2, have been fitted using equation (2) reported in [29] and [31], respectively. Note that MS-FMR measurements revealed the existence of small uniaxial in-plane anisotropy, note exceeding 60 Oe. The linear dependence of M_{eff} versus the inverse of the CoFeB effective thickness (shown in figure 2a) suggests the existence of surface magnetic anisotropy. $K_\perp$ could therefore be phenomenologically separated in volume (K_v) and interface (K_s) contributions and approximately obeying the relation: $K_\perp=K_v+K_s/t_{eff}$. The estimated interface anisotropy constants, deduced from the fit of MS-FMR (respectively BLS) data are 2.1±0.16 erg/cm^2 (1.9±0.17 erg/cm^2) and 0.97±0.09 erg/cm^2 for unbuffered and Ta-buffered CoFeB/TaO$_x$ systems, respectively. The slight difference between the MS-FMR and BLS (about 10%) is probably due to the difference in the applied magnetic field range when measuring the field dependence of the frequency, used to deduce M_{eff} and to the more unknown parameters implied in the fit of the BLS data to have M_{eff}. It is not easy to identify the exact mechanism behind this difference in K_s between Ta buffered and unbuffered CoFeB/TaO$_x$ but one should precise the higher substrate-induced roughness. Indeed, atomic force microscopy measurements (not shown here) for Si/SiO$_2$ substrate and the as grown Si/SiO$_2$/Ta(3nm) have shown that the RMS roughness decreases after the growth of Ta. Such roughness creates in-plane demagnetizing fields at edges of terraces reducing the shape anisotropy and therefore favors a higher interface PMA for CoFeB grown directly on Si/SiO$_2$.

It is worth mentioning the deviation of M_{eff} from the linear dependence for thinner CoFeB films (t_{eff} around 1.7 nm and 0.7 nm for unbuffered and Ta buffered systems) most probably due to the degradation of thinner CoFeB layers and the resulting lower Curie temperature. Therefore, although growing CoFeB directly on Si/SiO$_2$ increases drastically K_s, the sample quality degrades rapidly as CoFeB thickness decreases, making Ta buffer layer critical to develop spontaneously perpendicularly magnetized systems.

MS-FMR was used to measure the Gilbert damping (α) for CoFeB/TO$_x$ and Ta/CoFeB/TO$_x$ by investigating the frequency dependence of the half width at half maximum height (ΔH). The magnetic field was applied in the film plane direction, giving the minimal ΔH (determined from the variation of ΔH versus the in-plane magnetic applied field direction). α was then deduced from the linear fit of the frequency dependence of ΔH. For both systems, α varies linearly with $1/t_{eff}$ due the spin pumping, as shown in figure 2b. From the linear fit of these experimental data, it is then possible to determine values of CoFeB Gilbert damping α_{CFB} and effective spin mixing

conductance $g_{eff}^{\uparrow\downarrow}$ from the vertical axis intercept and the slope, respectively [29]. The obtained values of α_{CFB} and $g_{eff}^{\uparrow\downarrow}$ are (2.1±0.4)×10^{-3}, (3.1±0.19)×10^{-3}, (16.4±2.1) and (14.5±1.2) nm^{-2} for CoFeB/TaO$_x$ and Ta/CoFeB/TaO$_x$, respectively. The lower (higher) value of α_{CFB} ($g_{eff}^{\uparrow\downarrow}$) of CoFeB/TaO$_x$ compared to that of Ta/CoFeB/TaO$_x$ are in line with the conclusion drawn above on the improvement of K_s for the unbuffered CoFeB/TaO$_x$. Moreover, the intermixing between the CoFeB and Ta at the lower interface could result in a relatively wide interface region which may kill the abrupt potential change, and conduction electrons across the CoFeB/Ta interface are less scattered, resulting in small interface spin losses for Ta/CoFeB/TaO$_x$ system, as reported by Ta et al [32].
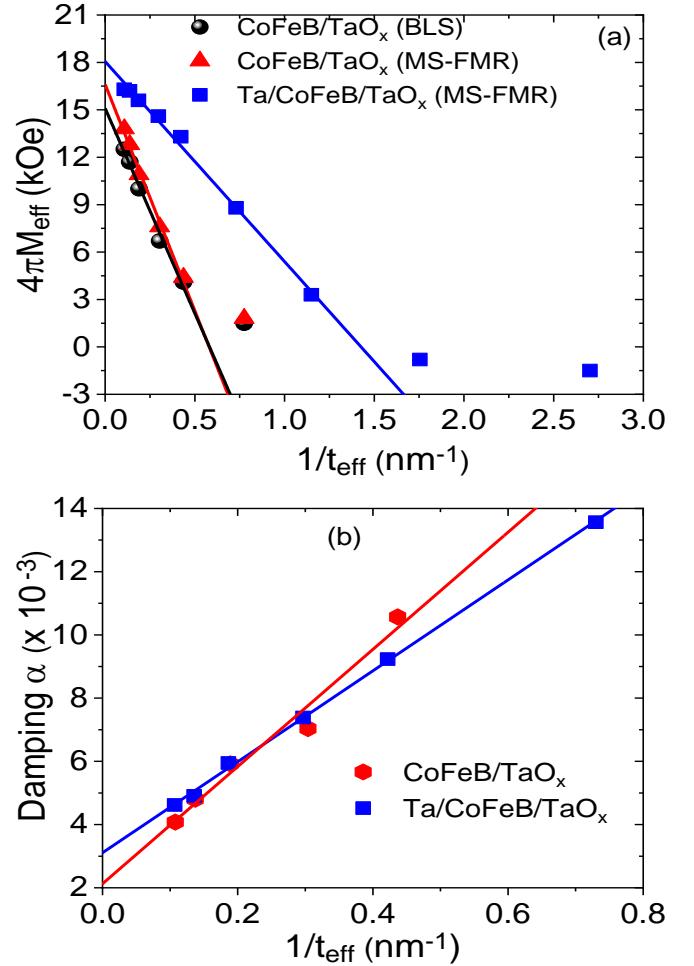

Fig. 2. (a) Effective magnetization ($4\pi M_{eff}$) and (b) Gilbert damping constant as a function of the inverse effective thickness of CoFeB films for CoFeB/TO$_x$ and Ta/CoFeB/TO$_x$ systems. $4\pi M_{eff}$ values have been extracted from the fit of the in-plane applied magnetic field dependence of spin waves frequency measured by MS-FMR and BLS. Symbols refer to experimental data and solid lines are linear fits.

B. 1- Effect of PtO$_x$ thickness

In the above investigation, the iDMI was not discussed due to its weak value in the TaO$_x$-based systems [29]. Therefore, the effect of oxidization on iDMI will be addressed for as grown and 225°C annealed PtO$_x$-based samples without Ta buffer layer owing to the strong iDMI generated by Pt. The variation of the Pt thickness to be oxidized is powerful method to change

the degree of oxidation at CoFeB/PtO interface. Therefore, CoFeB(1.5nm)/ PtO$_x$(t$_{Pt}$) grown directly on Si/SiO$_2$ substrates are considered in this study. For such ultrathin CoFeB films, BLS, in Damon-Eshbach configuration, has been used to investigate damping, PMA and iDMI. For iDMI, the thermally excited SW spectra have been recorded under in-plane saturating magnetic field, for each k$_{SW}$ within the range 4.1-20.45 µm^{-1} and then fitted with a Lorentzian. The linear fit of the k$_{SW}$ dependence of the frequency mismatch $\Delta F = F_S - F_{aS}$ was used to determine the iDMI strength, characterized by the effective constant D$_{eff}$ as given by equation (1).

$$\Delta F = F_S - F_{aS} = D_{eff} \frac{2\gamma}{\pi M_s} k_{SW} = \frac{D_S}{t_{eff}} \frac{2\gamma}{\pi M_s} k_{SW} \qquad (1)$$

For PMA and damping, the recorded spectra at k$_{SW}$=4.1 µm^{-1} and under variable in-plane applied magnetic fields were fitted with a Lorentzian to extract frequencies and the full width at half maximum linewidth (δF) for S and aS lines. To cancel iDMI contribution, the mean values of frequencies and δF of S and aS lines were considered to deduce K$_\perp$ and α, respectively. Figure 3, shows the nominal Pt thickness (which is then oxidized) dependence of the obtained values of K$_\perp$, α and D$_{eff}$ using $\gamma/2\pi$=30.27 GHz/T and M$_s$ =1520 emu/cm^3. Note the similar behaviors of K$_\perp$, α and D$_{eff}$ for as deposited and annealed samples. K$_\perp$ and α (see figure 3b) decreases significantly with increasing t$_{Pt}$. This is consistent with the increase of the CoFeB effective thickness. Indeed, when t$_{Pt}$ increases CoFeB is less oxidized, t$_d$ is reduced and consequently t$_{eff}$ is enhanced as confirmed by the increasing of the areal magnetic moment shown in the inset of figure 3a. It is well known that D$_{eff}$ varies linearly with 1/t$_{eff}$ for sufficient t$_{eff}$. However, when the FM thickness is lower than a critical value, D$_{eff}$ decreases with 1/t$_{eff}$ since iDMI requires a finite thickness for its full emergence and thus its magnitude is maximized [33]. Therefore, owing to the thick t$_d$ in CoFeB/PtO$_x$ systems and the 1.5 nm nominal thickness of CoFeB, t$_{eff}$ should be largely below 1 nm and thus D$_{eff}$ should increase with t$_{Pt}$ as explained above. To validate this hypothesis, the t$_{eff}\times$M$_s$ deduced from the VSM measurements (inset figure 3a) have been used in equation 1 to evaluate D$_s$. as shown in the inset of figure 3c. The variation of D$_s$ shows that t$_{eff}$ increases but remains lower than the critical value above which D$_s$ should be constant. Conversely $g_{eff}^{\uparrow\downarrow}$, deduced from damping values using α_{CFB}= 2.1×10^{-3}, t$_{eff}\times$M$_s$ and equation (4) reported in [30], is nearly constant as expected, confirming the peculiar behavior of D$_{eff}$ below the iDMI full emergence thickness.

Note that for annealed samples with PtO$_x$ thicknesses below 1 nm, no signal has been detected, suggesting that such samples are not magnetic at room temperature, likely because of an increased oxidation of CoFeB layer after annealing. Furthermore, annealing increases K$_\perp$ and α while t$_d$ and D$_{eff}$ are only slightly affected suggesting an enhancement of the CoFeB crystallinity and interfaces.

It is worth mentioning that linear correlation between K$_\perp$ and α (not shown here) was obtained for both Ta/CoFeB(tCoFeB)/TaOx, CoFeB(tCoFeB)/TaOx and as grown CoFeB(tCoFeB)/PtOx due to the second order the

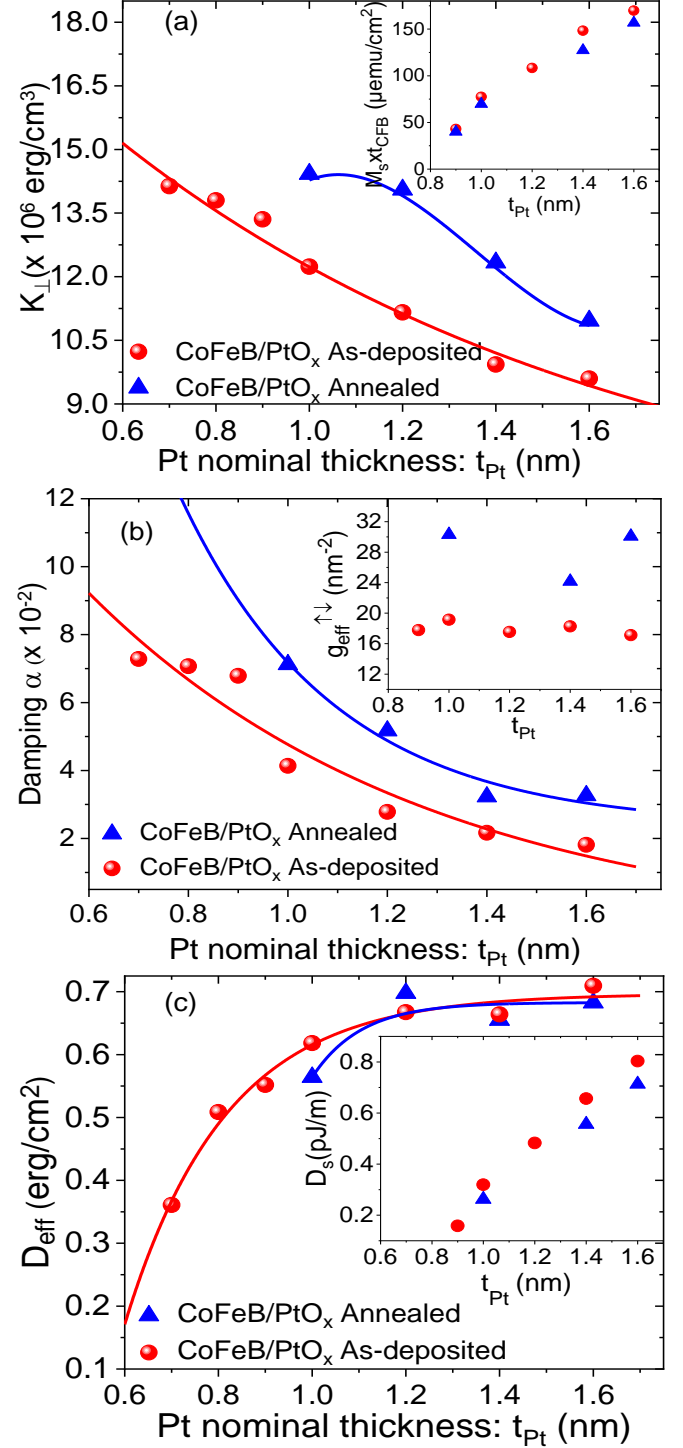dependence of the two parameters with SOC as expected theoretically.

Fig. 3. Variations of (a) perpendicular anisotropy constant (K$_\perp$), (b) Gilbert damping and (c) effective iDMI constant (D$_{eff}$) as a function of the nominal Pt thickness (t$_{Pt}$) for the as grown and the 225 °C annealed CoFeB(1.5 nm)/PtO$_x$ films. PtO$_x$ is obtained by oxidization of Pt t$_{Pt}$ indicated in the horizontal axis. Symbols refer to experimental data and solid lines are eye guides. Insets shows (a) areal magnetic moment, (b) effective spin mixing conductance and (c) surface iDMI constant versus t$_{Pt}$.

IV. CONCLUSION

We demonstrated that the underlayer nature and the capping layer thickness play a decisive role in tuning PMA, iDMI and

spin pumping-induced damping, confirming their interfacial origin and their spin-orbit coupling correlation. Indeed, large surface PMA was found in the unbuffered $CoFeB/TaO_x$ system and degraded for ultra-thin CoFeB films, making Ta buffer layer critical to develop spontaneous perpendicularly magnetized systems probably due to the different substrate induced roughness. The effect of PtO_x thickness on PMA, iDMI and spin pumping induced damping was investigated in as-deposited and 225°C annealed $CoFeB/PtO_x$ systems: a strong dependence of these three parameters with PtO_x thickness was observed. This was mainly attributed to variation of the dead layer, giving another opportunity to control these parameters depending on the desired application.

REFERENCES

[1] M. N. Baibich, J. M. Broto, A. Fert, F. Nguyen Van Dau, F. Petro, P. Etienne,G. Creuzet, A. Friederich, and J. Chazelas, "Giant Magnetoresistance of (001) Fe/ (001) Cr Magnetic Superlattices," *Phys. Rev. Lett.*, vol. 61, (21), pp. 2472-2475, 1988.

[2] G. Binasch, P. Grünberg, F. Saurenbach, and W. Zinn, "Enhanced magnetoresistance in layered magnetic structures with antiferromagnetic interlayer exchange," *Physical Review B*, vol. 39(7), pp. 4828-4830, 1989.

[3] B. Tudu and A. Tiwari, "Recent Developments in Perpendicular Magnetic Anisotropy Thin Films for Data Storage Applications," *Vacuum*, vol. 146, pp. 329-341, 2017.

[4] J.G. Zhu and C. Park, "Magnetic tunnel junctions," *Materialstoday*, vol. 9(11), pp. 36-45, 2006.

[5] A. Fert, N. Reyren and V. Cros, "Magnetic skyrmions: advances in physics and potential applications," *Nat. Mat.*, vol. 2, pp. 17031, 2017.

[6] X. Zhang , Y. Zhou , K. Mee Song, T-E. Park, J. Xia, M. Ezawa, X. Liu, W. Zhao, G. Zhao and S. Woo, "Skyrmion-electronics: writing, deleting, reading and processing magnetic skyrmions toward spintronic applications," *J. Phys.: Condens. Matter*, vol. 32, pp. 143001, 2020.

[7] M. T. Johnson, P. J. H. Bloemenz, F. J. A. den Broeder, and J. J. de Vries, "Magnetic anisotropy in metallic multilayers*," Rep. Prog. Phys.,* vol. 59, pp. 1409, 1996.

[8] A. Brataas, Y. Tserkovnyak, G. E .W. Bauer and B. I Halperin, "Spin battery operated by ferromagnetic resonance," *Phys. Rev. B*, vol. 66, pp. 060404, 2002.

[9] Y. Tserkovnyak, A. Brataas, G. E .W. Bauer and B. I Halperin, "Nonlocal magnetization dynamics in ferromagnetic heterostructures", Rev. Mod. Phys., vol. 77, pp. 1375, 2005.

[10] I. Dzyaloshinsky, "A thermodynamic theory of weak ferromagnetism of antiferromagnetics," *J Phys. Chem.* Sol, vol. 4, pp. 241-255, 1958.

[11] T. Moriya, "New Mechanism of Anisotropic Superexchange Interaction," *Phys. Rev. Lett*., vol. 4, pp. 228, 1960.

[12] S. Bhatti, R. Sbiaa, A. Hirohata, H. Ohno, S. Fukami, and S.N. Piramanayagam, "Spintronics based random access memory: a review," *Materials today*, vol. 20, pp. 530-548, 2017..

[13] B. Rodmacq, S. Auffret, B. Dieny, S. Monso, and P. Boyer, "Crossovers from in-plane to perpendicular anisotropy in magnetic tunnel junctions as a function of the barrier degree of oxidation," *J. Appl. Phys.*, vol. 93, pp. 7513, 2003.

[14] B. Dieny and M. Chshiev,"Perpendicular magnetic anisotropy at transition metal/oxide Interfaces and applications," *Rev. Mod. Phys.*, vol. 89, pp. 025008, 2017.

[15] S. Ikeda, J. Hayakawa, Y. Min Lee, F. Matsukura, Y. Ohno, T. Hanyu, and H. Ohno, "Magnetic tunnel junctions for spintronic memories and beyond," *IEEE Trans. Elec. Dev.*, vol. 54 (5), pp. 991-1002, 2007.

[16] S. Peng, D. Zhu, J. Zhou, B. Zhang, A. Cao, M. Wang, W. Cai, K. Cao, and W. Zhao, "Modulation of heavy metal/ferromagnetic metal Interface for high-performance spintronic devices,". *Adv. Electron. Mater.*, vol. 5, pp.1900134, 2019.

[17] D. M. Lattery, D. Zhang, J. Zhu, X. Hang, J-P. Wang and X. Wang, "Low Gilbert Damping Constant in Perpendicularly Magnetized W/CoFeB/MgO Films with High Thermal Stability," *Sc. Rep.*, vol. 8, pp. 13395, 2018.

[18] M. Uchida, Y. Onose, Y. Matsui, and Y. Tokura, "Real-Space Observation of Helical Spin Order ," *Science*, vol. 311, pp.359-361 2006.

[19] M. Bode, M. Heide, K. von Bergmann, P. Ferriani, S.Heinze, G. Bihlmayer, A. Kubetzka, O. Pietzsch, S. Blügel, and R. Wiesendanger, "Chiral magnetic order at surfaces driven by inversion asymmetry ," *Nature*, vol. 447, pp. 190, 2007.

[20] A. Tonomura, X. Yu, K. Yanagisawa, T. Matsuda, Y. Onose, N. Kanazawa, H. S. Park and Y. Tokura, "Real-Space Observation of Skyrmion Lattice in Helimagnet MnSi Thin Samples," *Nano Lett.,* vol. 12, pp. 1673−1677, 2012.

[21] A. Fert, V. Cros and J. Sampaio, "Skyrmions on the track," *Nat. nanotech.*, vol. 8, pp. 152-156, 2013.

[22] A. Thiaville, S. Rohart, E. Jué, V. Cros, and A. Fert, "Dynamics of Dzyaloshinskii domain walls in ultrathin magnetic films," *EPL*, vol. 100, pp. 57002, 2012.

[23] H. X. Yang, O. Boulle, V. Cros, A. Fert, and M. Chshiev,"Controlling Dzyaloshinskii-Moriya Interaction via Chirality Dependent Atomic-Layer Stacking, Insulator Capping and Electric Field," *Sci. Rep.,* vol. 8, pp. 12356, 2018.

[24] A. Belabbes, G. Bihlmayer, S. Blügel, and A. Manchon, "Oxygen-enabled control of Dzyaloshinskii-Moriya Interaction in ultra-thin magnetic films," *Sci. Rep.,* vol.6, pp. 24634, 2016.

[25] H. T. Nembach, E. Jué, E. R. Evarts and J. M. Shaw, "Correlation between Dzyaloshinskii-Moriya interaction and orbital angular momentum at an oxide-ferromagnet interface," *Phys. Rev. B*, vol. 101, pp. 020409(R), 2020.

[26] M. Arora, J. M. Shaw and H. T. Nembach, "Variation of sign and magnitude of the Dzyaloshinskii-Moriya interaction of a ferromagnet with an oxide interface," *Phys. Rev. B*, vol. 101, pp. 054421, 2020.

[27] T. Srivastava, M. Schott, R. Juge , V. Křižáková, M. Belmeguenai, Y. Roussigné, A. Bernand-Mantel, L.t Ranno, S. Pizzini, S-M. Chérif, A. Stashkevich, S. Auffret, O. Boulle,G. Gaudin, M. Chshiev, C. Baraduc, H. Béa, "Large-Voltage Tuning of Dzyaloshinskii-Moriya Interactions: A Route toward Dynamic Control of Skyrmion Chirality," *Nano Lett.* vol., 18, pp. 4871–4877, 2018.

[28] T. Srivastava, W. Lim, I. Joumard, S. Auffret, C. Baraduc and H. Béa, "Mapping different skyrmion phases in double wedges of Ta/FeCoB/TaOx trilayers," *Phys. Rev. B*, vol. 100, pp. 220401(R), 2019.

[29] I. Benguettat-El Mokhtari, Y. Roussigné, S. M. Chérif, A. Stashkevich, S. Auffret, C. Baraduc, M. Gabor, H. Béa, and M. Belmeguenai, "Interface phenomena in ferromagnet/TaOx-based systems: Damping, perpendicular magnetic anisotropy, and Dzyaloshinskii-Moriya interaction," *Phys. Rev. Mat.*, vol. 4, pp. 124408, 2020.

[30] C. Le Graët, D. Spenato, N. Beaulieu, D. Dekadjevi, J-Ph. Jay, S. Pogossian, B. Warot-Fonrose, J. Ben Youssef, "Driving mechanism for damping and g-factor innon-amorphous ferromagnetic CoFeZr ultrathin films," *EuroPhys. Lett*., vol. 115, pp. 17002, 2016.

[31] I. Benguettat-El Mokhtari, D. Ourdani, Y. Roussigné, R. B. Mos, M. Nasui, F. Kail, L. Chahed, S. M. Chérif, A. Stashkevich, M. Gabor, nd M Belmeguenai, "Perpendicular magnetic anisotropy and interfacial Dzyaloshinskii–Moriya interaction in as grown and annealed X/Co/Y ultrathin systems," *Phys.: Condens. Matter*, vol. 132, pp. 495802, 2020.

[32] X. Tao, Q. Liu, B. Miao, R. Yu, Z. Feng, L. Sun, B. You, J. Du, K. Chen, S. Zhang, L. Zhang, Z. Yuan, D. Wu, H. Ding, *Sci. Adv.* Vol. 4, pp.eaat1670, 2018.

[33] Y-K. Park, J-S. Kim, Y-S. Nam, S. Jeon, J-H. Park, K-W. Kim, H-W. Lee, B-C. Min, and S-B. Choe, "Interfacial atomic layers for full emergence of interfacial Dzyaloshinskii–Moriya interaction," *NPG Asia Materials*, vol. 12, pp. 38, 2020.